Journal of Power Sources 187 (2009) 80–84

Contents lists available at ScienceDirect

Journal of Power Sources

journal homepage: www.elsevier.com/locate/jpowsour

Short communication

Preparation and characterization of carbon-supported sub-monolayer palladium decorated gold nanoparticles for the electro-oxidation of ethanol in alkaline media

L.D. Zhu, T.S. Zhao*, J.B. Xu, Z.X. Liang

Department of Mechanical Engineering, The Hong Kong University of Science and Technology, Clear Water Bay, Kowloon, Hong Kong SAR, China

ARTICLE INFO

Article history:
Received 1 July 2008
Received in revised form 3 September 2008
Accepted 16 October 2008
Available online 6 November 2008

Keywords:
Electrocatalyst
Palladium
Gold
Ethanol
Alkaline
Fuel cell

ABSTRACT

Carbon-supported gold nanoparticles (Au/C) are successfully decorated with mono- or sub-monolayer palladium atoms with different Pd/Au atomic ratios by a chemically epitaxial seeded growth method. TEM, UV–vis spectrometry and XRD techniques are used to characterize the particle size, dispersion, palladium coverage on gold seeds and crystal structures of the prepared catalysts. Cyclic voltammetric tests show that the Pd-decorated Au/C (denoted by Pd@Au/C) have higher specific activities than that of Pd/C for the oxidation of ethanol in alkaline media. This suggests that the Pd utilization is improved with such a surface-alloyed nanostructure. In addition, stable chronoamperometric responses are achieved with the so-prepared electrocatalysts during ethanol oxidation.

1. Introduction

During the past decade, direct alcohol fuel cells (DAFCs), typically with either methanol or ethanol as the fuel, have been widely recognized as very attractive and potential power sources for portable electronic devices and other mobile applications [1–4]. As the simplest alcohol, methanol has been extensively investigated as the fuel of direct methanol fuel cells (DMFCs) [5]. In addition to other technical problems encountered in the development of DMFCs, however, the toxicity of methanol may limit the wide application of this type of fuel cell. By comparison, in terms of its much lower toxicity, higher energy density (8.01 kWh kg^{-1}), and the fact that it can be massively produced from agricultural products and the fermentation of sugar-containing raw materials (biomass), ethanol is a more suitable fuel for fuel cells in both portable and mobile applications.

Up to now, most of the direct ethanol fuel cells (DEFCs) have been operated under acidic conditions with a proton-exchange membrane, e.g., Nafion, as the electrolyte. In such a strong acidic medium, platinum or platinum-based electrocatalysts are usually required. As platinum is expensive and rare, the cost of fuel cells with this type of electrocatalyst is high. In addition, the sluggish kinetics of the ethanol oxidation reaction (EOR) is another problem that limits the widespread commercialization of DEFCs with acid electrolyte membranes. By contrast, in the fuel cells with alkaline electrolyte membranes, both the EOR and the oxygen reduction reaction (ORR) are relatively easier, making it possible to use non-platinum catalysts in DEFCs. As a result, the cost of alkaline DEFCs can be reduced [6,7].

Traditional alkaline fuel cells (AFCs) use an aqueous potassium hydroxide (KOH) solution as the electrolyte to conduct anions (OH^-) produced at the cathode. Such an operating scheme always suffers from a major operating constraint caused by carbon dioxide contamination because this gas reacts with OH^- to form a carbonate precipitate. This phenomenon, which is termed 'carbonation', leads to potential blockage of the electrolyte pathways and/or electrode pores [7]. As such, alcoholic fuels are rarely utilized as the fuel for AFCs that use aqueous KOH solution as the electrolyte, instead highly purified hydrogen and oxygen are employed. To alleviate the contamination of CO_2, several strategies have been proposed, for example, circulating electrolyte, scrubbing CO_2 using soda lime, and the use of solid-state electrolytes (anion-exchange membranes) [8,9]. In particular, development of the anion-exchange membrane makes it possible to use alcohols as the fuel for AFCs. Consequently, some alkaline DAFC systems with anion-exchange membranes have recently been demonstrated [10–15].

* Corresponding author. Tel.: +852 2358 8647.
E-mail address: metzhao@ust.hk (T.S. Zhao).

0378-7753/$ – see front matter © 2008 Elsevier B.V. All rights reserved.
doi:10.1016/j.jpowsour.2008.10.089

Most of the existing alkaline DAFCs still use Pt or Pt alloys to form electrocatalysts, which incurs the cost problem mentioned earlier. Recently, Chen et al. [16] discovered that Pd had a higher activity than Pt with respect to the EOR in a basic medium. This suggests that Pd is a promising alternative candidate to Pt as the electrocatalyst for alkaline DEFCs. Shen et al. [17–21] developed a series of Pd and Pd alloy electrocatalysts supported with various materials for the EOR. They found that the activity of Pd was influenced by the additive moiety and the support material, which indicates a synergetic effect of the additive or support with Pd on the EOR in the alkaline medium. Nevertheless, the loading of Pd used in the above cases is still too high for commercial applications. Hence, further effort to develop more active and cheaper electrocatalysts for the EOR is necessary.

The objective of this work is to prepare a carbon-supported Pd-decorated Au nano-electrocatalyst for the EOR in an alkaline medium. The work is motivated by the following idea. Since the electrochemical reaction occurs just at the surface of Pd, the loading of Pd can be reduced by using a relatively cheaper and more abundant metal (e.g., Au) nanoparticle as a second-grade support, on which Pd atoms are deposited as monolayer or sub-monolayer adatoms by chemical or electrochemical (under potential deposition) epitaxial growth methods. This study reports the preparation and characterization of Pd-decorated Au nanoparticles supported on carbon with different Au to Pd ratios. The pendings show that the developed non-Pt nanocatalyst has high specific activity and stable performance for the EOR in an alkaline medium.

2. Experimental

2.1. Chemicals

Metal precursors, including gold chloride and palladium chloride, were purchased from Sigma–Aldrich Corp. Trisodium citrate, sodium borohydride, ascorbic acid, ethanol, and potassium hydroxide (all from Merk KGaA) were used as-received. Vulcan XC-72 carbon (particle size 30–50 nm) was provided by the E-TEK Company. 0.25 mM $HAuCl_4$ and 1 mM $HPdCl_4$ solutions were prepared by dissolving suitable amounts of gold chloride and palladium chloride in hydrochloride acid solution.

2.2. Synthesis of carbon-supported Pd@Au nanoparticles

The Pd-decorated Au nanoparticles (denoted by Pd@Au) were prepared by nano-Au seed mediated epitaxial growth. Briefly, the nano-Au seeds were first prepared by the reduction of 0.25 mM of $AuCl_4^-$ ions with excess sodium borohydride in the presence of 0.25 mM trisodium citrate as the stabilizing reagent in an ice-water bath with stirring. The Au colloidal seeds (hydrosol) were stored at 4 °C until used and remained stable at least 3 months. Palladium was then deposited on the Au seeds via the following procedure. A certain amount of the Au hydrosol was mixed with different volumes of 1.0 mM H_2PdCl_4 and cooled in an ice-water bath. Then, an excess of ascorbic acid was slowly dropped into the mixture while stirring. The colour of the mixture turned to black-brown within minutes. Stirring was maintained for a further 30 min after finishing the addition of ascorbic acid. The resulting Pd@Au hydrosols were then deposited on Vulcan-72 active carbon black to give a total metal loading of 20 wt.%. In practice, a certain amount of Vulcan XC-72 was dispersed in water and dropped on the prepared hydrosols. The mixture was then stirred for 24 h. The suspension was filtered and washed with copious water. The filtrate was dried at 70 °C under vacuum over night. For comparison, 20 wt.% of Pd/C and Au/C were also prepared according to the procedures detailed elsewhere [22,23].

2.3. Characterization of Pd@Au nanoparticles

The UV–vis spectra of the Au and Pd@Au hydrosols were obtained with a Lambda 20 model spectrophotometer (Perkin-Elmer) equipped with quartz cells. The concentration of Au in the Au and Pd@Au hydrosols was 0.25 mM. The particle sizes and morphologies of the carbon-supported Pd@Au nanoparticles (Pd@Au/C) were characterized by means of a JEOL 2010 transmission electron microscope (TEM) at 200 kV. The X-ray diffraction (XRD) patterns for the catalysts were obtained with a Philips powder diffraction system (model PW 1830) using a Cu Kα source operating at 40 keV at a scan rate of $0.025^\circ\ s^{-1}$. XPS measurements of the catalysts were carried out with a Physical Electronics PHI 5600 multi-technique system using an Al monochromatic X-ray at a power of 350 W.

Electrochemical measurements were conducted with a conventional three-electrode glass cell under the control of an EG&G PAR potentiostat/galvanostat (Model 273A). A platinum gauze and a saturated calomel electrode (SCE) served as the counter and the reference electrodes, respectively. All potentials are reported with respect to the SCE. The working electrode was a 3-mm glassy carbon electrode (GCE) modified with the carbon-supported nanoparticles. This was achieved by dropping a suitable amount of ethanol-dispersed electrocatalyst on the GCE. Cyclic voltammetric and chronoamperometric experiments were performed in 1 M KOH aqueous solution in the absence and presence of 1 M ethanol at ambient temperature (20 ± 0.5 °C). High purity of nitrogen was used for solution deaeration.

3. Results and discussion

The Pd@Au nanoparticles were prepared with successive procedures, in which Au seeds with a mean size of 4.0 nm (measured from the TEM image) were first synthesized and then palladium was deposited on the surface of Au through a chemically epitaxial growth strategy. To verify whether the palladium was coated on the Au nanoparticles instead of forming new nuclei, UV–vis spectroscopy was employed because it is well understood that the Au hydrosol exhibits a strong absorption peak at around 510 nm due to the surface plasmon resonance (SPR) of Au nanoparticles. The absorption spectra of the Au and Pd@Au hydrosols are presented in Fig. 1. An absorption peak positioned at ca. 509 nm can be clearly observed for the Au hydrosol and is ascribed to the SPR

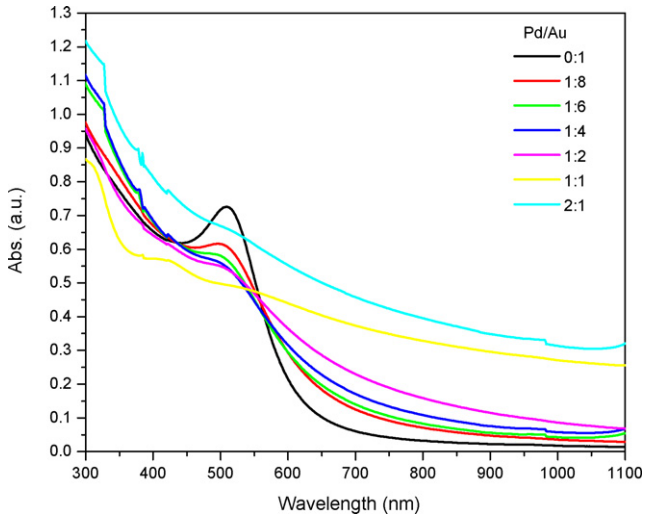

Fig. 1. UV–vis absorption spectra of Au and Pd@Au hydrosols.

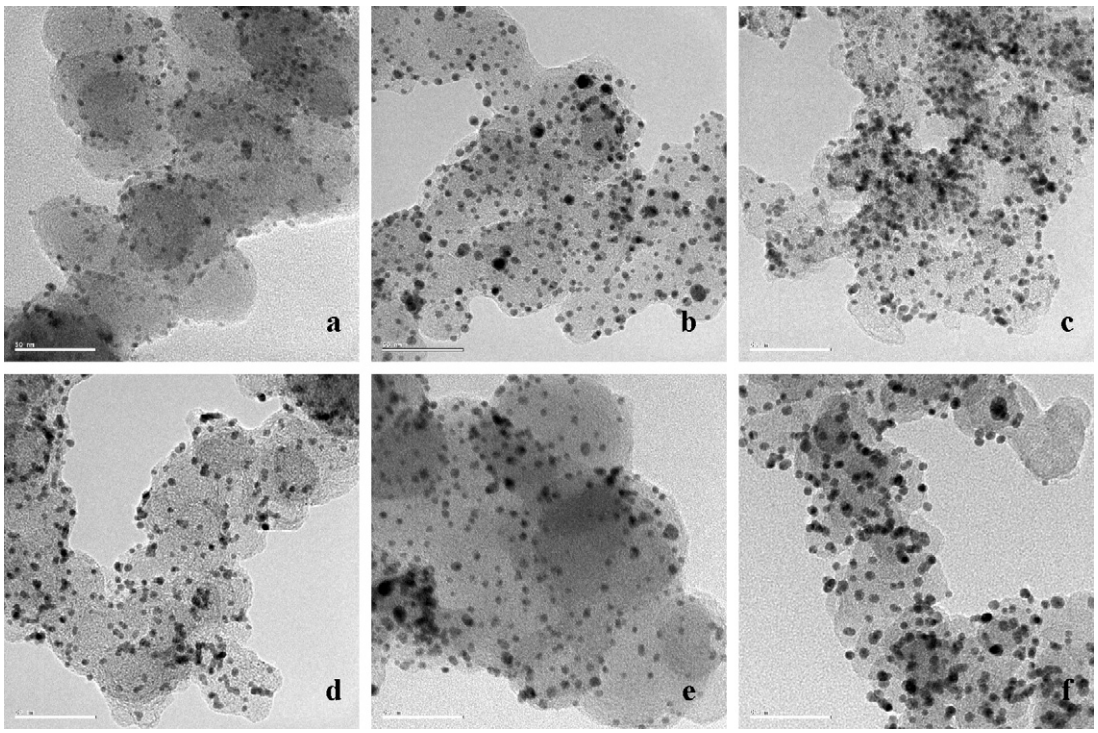

Fig. 2. TEM images of (a) Pd/C, (b) Au/C, and Pd@Au/C with Pd/Au ratio of (c) 1:6, (d) 1:4, (e) 1:2 and (f) 1:1. Scale bar equals 50 nm.

of nano-Au. When palladium is deposited on the surface of Au, however, the naked surface area of nano-Au decreases so as to diminish the absorption intensity. With increase in the Pd:Au ratio, the absorption intensity of the Pd-decorated hydrosols decreases accordingly. When the ratio approaches 1:2, the Au SPR peak is dramatically suppressed and shifts to a lower wavelength located at 500 nm. Similar behaviour has been reported elsewhere [24]. With further increase in the Pd:Au ratio, for instance, to 1:1 or larger (2:1), the Au SPR absorption peak disappears. This indicates that the Au nanoparticles are totally encapsulated by the surrounding Pd adatoms.

The carbon-supported Pd, Au and Pd@Au nanoparticles were then characterized by TEM to determine the morphology, dispersion and particle size of the prepared electrocatalysts. As shown in Fig. 2, all the synthesized nanoparticles are well dispersed with negligible agglomeration and have a narrow size-distribution, as the result of the stabilizing effect of the acetate ions. The average nanoparticle size measured from counting about 100 individual particles is about 4.2, 4.0, 4.0, 4.1, 4.6 and 5.4 nm for Pd, Au, Pd@Au (1:6), Pd@Au (1:4), Pd@Au (1:2) and Pd@Au (1:1), respectively. Apparently, with increase in the Pd:Au ratio, the particle size (diameter) increases accordingly, further demonstrating that Pd grows epitaxially on the surface of Au seed, rather than forming a new nucleus. It is difficult, however, to discern the core–shell components from the TEM images because Au and Pd possess the same crystal structure and display similar imaging contrast.

The XRD patterns of the carbon-supported Pd, Au and Pd@Au electrocatalysts are given in Fig. 3. All the XRD patterns of the Pd@Au/C are identical to that of the pure Au/C and the resulting diffraction peaks located at 2θ values of 37.5°, 44.3°, 64.8° and 77.8° are attributed to the (1 1 1), (2 0 0), (2 2 0) and (3 1 1) planes of Au, respectively [25]. These peaks indicate that Au in the Pd-decorated nanoparticles is all present in the face-centered cubic (fcc) structure. Compared with the XRD pattern of Pd/C, no diffraction peaks assigned to Pd are evident in those of Pd@Au/C electrocatalysts, suggesting the absence of large isolated Pd particles. This finding further demonstrates that Pd is mainly deposited on the surface of the Au seeds as a thin shell layer rather than forming a new nucleus. It is also observed that the intensities of the diffraction peaks of Au decrease gradually with increase in Pd loading. This may be ascribed to an enhanced the Pd coverage and thickness of the Pd atomic layer decorated on the Au seeds that hinders the penetration depth of X-rays.

The electrocatalytic activities of the Pd@Au/C were investigated with 1 M ethanol/KOH solution at room temperature. Fig. 4a shows the CV curves obtained for electrocatalyst-coated electrodes with the same total metal loading in 1 M ethanol/KOH. Clearly, the EOR at Au/C has more positive onset and peak potentials, which suggests that the electrode kinetics are more sluggish on

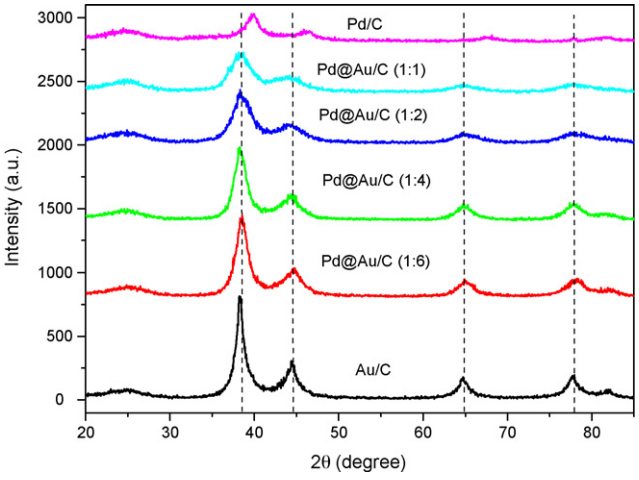

Fig. 3. XRD patterns of Pd/C, Au/C and Pd@Au/C catalysts.

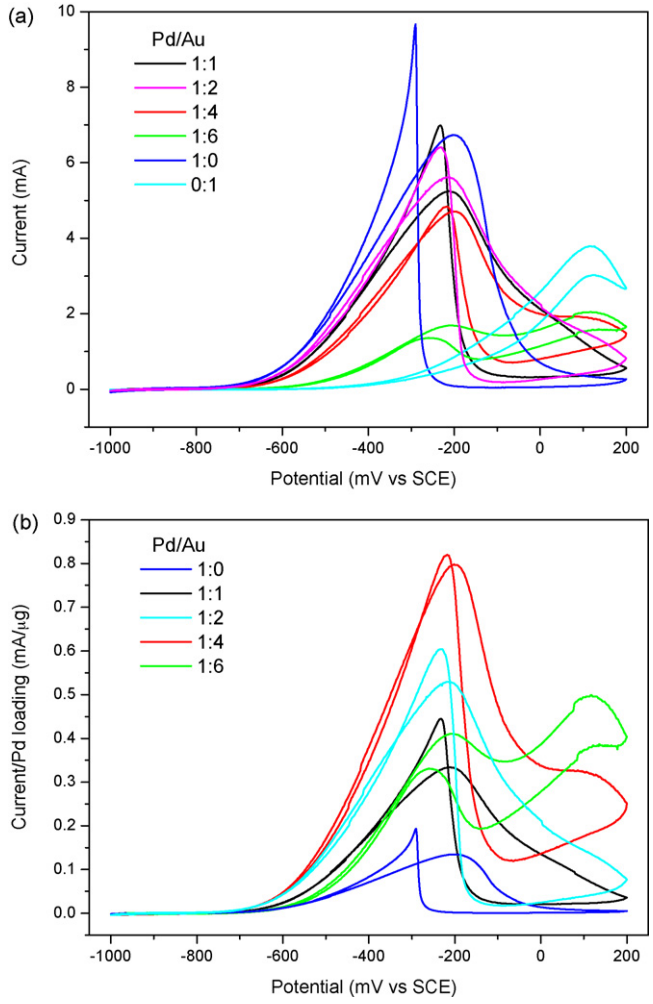

Fig. 4. Cyclic voltammograms of Pd/C, Au/C and Pd@Au/C with (a) same total metal loading and (b) specified Pd loading in 1 M ethanol + 1 M KOH at scan rate of 50 mV s^{-1}.

Au/C than on Pd@Au/C. The peak current of the forward scan for Pd@Au/C increases as the Pd loading decorated on Au is increased in the Pd:Au ratio from 1:6 to 1:1. This behaviour is attributed to an improvement in the electroactive surface area of Pd. When the Pd:Au ratio reaches 2:1, however, the peak current decreases slightly. This may be due to an increase in particle size.

The most significant merit of the prepared Pd-decorated Au catalyst is that the utilization of active metal (i.e., Pd) becomes enhanced. From the CVs in Fig. 4b, it is seen that the specific catalytic activity of Pd decreases with increase in the Pd:Au ratio from 1:4 to 1:1 if the peak current of the forward scan is taken to evaluate the performance of the electrocatalysts. In an electrochemical reaction, only the surface atoms are active as the catalyst, therefore, the more dispersed Pd atoms on the Au surface, the more specific activity will be achieved. For Pd@Au (1:1) with an average particle size of about 5.4 nm, corresponding shell thickness can be calculated to be about 0.7 nm, which equals to around two layers of Pd atoms by subtracting the Au seed size (average value of 4.0 nm). For the Pd@Au (1:2), however, the calculated shell thickness is only about 0.30 nm, matching the diameter of the Pd atom (0.35 nm) and suggesting that almost a monolayer of Pd atoms is decorated on the Pd@Au (1:2). Similarly, for nanoparticles with a Pd:Au ratio lower than 1:2, Pd atoms cannot fully cover the surfaces of the Au seeds and a sub-monolayer of Pd must therefore result. In this case,

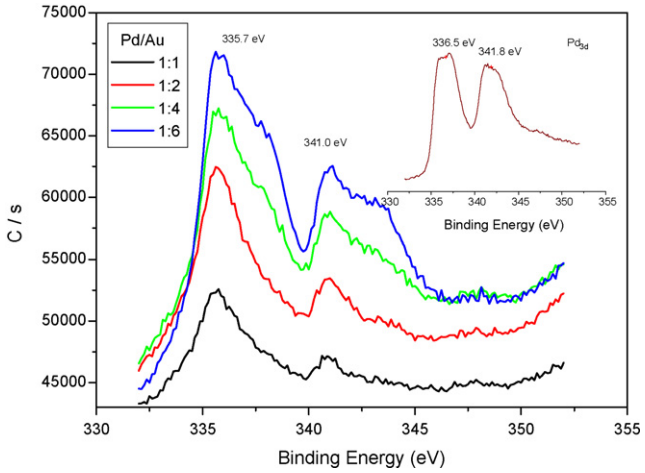

Fig. 5. XPS spectra of Pd_{3d} for Pd@Au/C catalysts. Inset shows the XPS spectra of Pd/C.

the dispersion of Pd would deteriorate with increasing Pd:Au ratio (from 1:4 to 1:1) due to the stacked Pd atoms and this would lower the utilization of the Pd catalyst. On the other hand, for a Pd:Au ratio of 1:6, the activity is slightly lower than the others, which may be ascribed to a sparsely distribution of Pd atoms on the surface of gold so that a continuous Pd sub-monolayer necessary for the dehydrogenation of ethanol [26] cannot be formed.

The peak current ratio of the forward to backward scans (I_b/I_f) is usually taken as the criterion to evaluate contamination arisen from poisoning species. From Fig. 4a, it is observed that the value of I_b/I_f (1.44) for Pd/C is larger than that of Pd-decorated Au/C (e.g., 1.12 for Pd@Au/C (1:2) and 1.01 for Pd@Au/C (1:4)), suggesting that poisoning of Pd/C is more serious than that of the Pd@Au/C. The anti-poison feature of Pd@Au/C is ascribed to the effect of the Au support which weakens the bonding interaction between the absorption species and Pd [27]. This point is further confirmed by XPS spectra, as displayed in Fig. 5. It can be seen that the binding energy peaks of Pd_{3d} are around 336.5–341.8 eV for pure Pd/C and negatively shift to about 0.5–0.8 eV after Pd is deposited on the Au seeds. As discussed earlier, the thickness of Pd atomic layer decorated on Au is no more than two atomic layers within which the electronic impact imposed by Au atoms is still effective [28]. There-

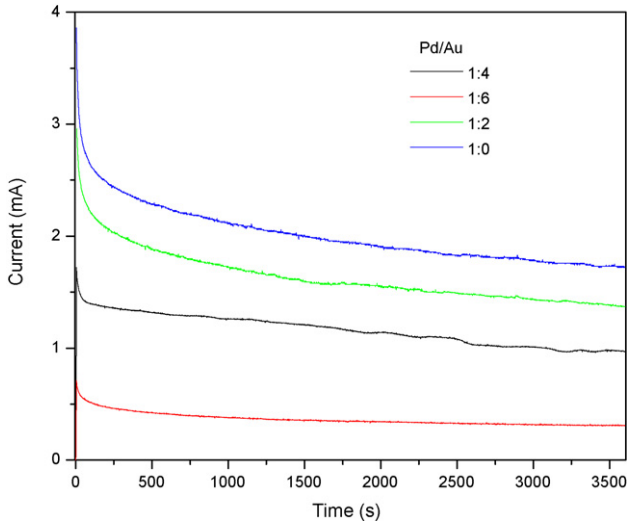

Fig. 6. Chronoamperograms of Pd/C and Pd@Au/C in 1 M ethanol + 1 M KOH at operation potential of −0.4 V.

fore, the negative binding energy shift must be related to electron donation from the d-orbital of Au which changes the electron cloud density of the Pd atom. Consequently, the absorptive strengths of the reaction intermediates in ethanol oxidation are significantly weakened. The chronoamperometric experiments shown in Fig. 6 indicate that the Pd activity towards the EOR in the alkaline medium is more stable after Pd is decorated on Au, which supports the electronic effect.

4. Conclusions

It has been shown that a monolayer or a sub-monolayer of Pd adatoms decorated Au/C can be easily synthesized by controlling the Pd:Au atomic ratio in the precursors via a chemically epitaxial growth method. The prepared electrocatalysts are well-dispersed and have narrow particle size distributions. Palladium is exclusively deposited on the nano-Au particles rather than forming new nuclei. With such a growth method, the loading of Pd is dramatically minimized so as to improve the specific activity of the catalysts for the EOR in the alkaline medium. Due to the electronic interaction between the Au support and the Pd decoration and the enhanced anti-poison capability for absorbed contamination species, Pd@Au/C shows more stable performance than pure Pd/C.

Acknowledgements

The work described in this paper was fully supported by a grant from the Research Grants Council of the Hong Kong Special Administrative Region, China (Project No. 622807) and by the Joint Research Fund for Hong Kong and Macao Young Scholars (Project No. 50629601).

References

[1] Y.L. Guo, Y.Z. Zheng, M.H. Huang, Electrochim. Acta 53 (2008) 3102–3108.
[2] C. Lamy, E.M. Belgsir, J.-M. LeGer, J. Appl. Electrochem. 31 (2001) 799–809.
[3] M.Y. Lo, I.H. Liao, C.C. Huang, Int. J. Hydro. Energy 32 (2007) 731–735.
[4] E. Antolini, J. Power Sources 170 (2007) 1–12.
[5] C. Lamy, A. Lima, V. LeRhun, F. Delime, C. Coutanceau, J. Leger, J. Power Sources 105 (2002) 283–296.
[6] Y. Wang, L. Li, L. Hu, L. Zhuang, J. Lu, B. Xu, Electrochem. Commun. 5 (2003) 662–666.
[7] G.F. McLean, T. Niet, S. Prince-Richard, N. Djilali, Int. J. Hydro. Energy 27 (2002) 507–526.
[8] P. Gouérec, L. Poletto, J. Denizot, E. Sanchez-Cortezon, J.H. Miners, J. Power Sources 129 (2004) 193–204.
[9] M. Cifrain, K.V. Kordesch, J. Power Sources 127 (2004) 234–242.
[10] A.Yu. Tsivadze, M.R. Tarasevich, B.N. Efremov, N.A. Kapustina, P.V. Mazin, Doklady Phys. Chem. 415 (2007) 234–236.
[11] K. Matsuoka, Y. Iriyama, T. Abe, M. Matsuoka, Z. Ogumi, J. Power Sources 150 (2005) 27–31.
[12] C.C. Yang, S.J. Chiu, W.C. Chien, J. Power Sources 162 (2006) 21–29.
[13] E.H. Yu, K. Scott, J. Power Sources 137 (2004) 248–256.
[14] E.H. Yu, K. Scott, J. Appl. Electrochem. 35 (2005) 91–96.
[15] J.S. Park, S.H. Park, S.D. Yim, Y.G. Yoon, W.Y. Lee, C.S. Kim, J. Power Sources 178 (2008) 620–626.
[16] Y. Chen, L. Zhuang, J. Lu, Chin. J. Catal. 28 (2007) 870–874.
[17] P.K. Shen, C.W. Xu, Electrochem. Commun. 8 (2006) 184–188.
[18] H.T. Zheng, Y.L. Li, S.X. Chen, P.K. Shen, J. Power Sources 163 (2006) 371–375.
[19] F.P. Hu, P.K. Shen, J. Power Sources 173 (2007) 877–881.
[20] M. Nie, H. Tang, Z. Wei, S.P. Jiang, P.K. Shen, Electrochem. Commun. 9 (2007) 2375–2379.
[21] C. Xu, Z. Tian, P.K. Shen, S.P. Jiang, Electrochim. Acta 53 (2008) 2610–2618.
[22] X. Wang, Y. Tang, Y. Gao, T. Lu, J. Power Sources 175 (2008) 784–788.
[23] W. Zhou, J. Lee, Electrochem. Commun. 9 (2007) 1725–1729.
[24] N. Kristianm, X. Wang, Electrochem. Commun. 10 (2008) 12–15.
[25] C. Xu, Z. Tian, Z. Chen, S.P. Jiang, Electrochem. Commun. 10 (2008) 246–249.
[26] B. Du, Y. Tong, J. Phys. Chem. B 109 (2005) 17775–17778.
[27] D.I. Enache, J. Edwards, P. Landon, B. Solsona-Espriu, A. Carley, A. Herzing, M. Watanabe, C.J. Kiely, D.W. Knight, G.J. Hutchings, Science 311 (2006) 362–365.
[28] J.W. Hu, Y. Zhang, J.F. Li, Z. Liu, B. Ren, S.G. Sun, Z.Q. Tian, T. Lian, Chem. Phys. Lett. 408 (2005) 354–359.